OPERATION AND PERFORMANCE OF A MEDIUM VOLTAGE DC LINK

Avinash AITHAL
Cardiff University - UK
AithalAV@cardiff.ac.uk

Jianzhong WU
Cardiff University - UK
WuJ5@cardiff.ac.uk

ABSTRACT

The operation of a voltage source converter (VSC) based Medium Voltage (MV) DC link is described. The use of a DC link in an MV distribution network is presented, considering salient similarities and differences to a high voltage (HV) DC link. A PSCAD/EMTDC model was used to demonstrate the dynamic operation of an MVDC link, under normal and faulted network conditions. The study shows that MVDC can provide flexibility in a distribution network by decoupling real (P) and reactive (Q) power flows through the link, under normal operation. During a fault however, the current injected from the converter could interfere with the detection and discrimination of AC system faults, in distribution networks with current based protection scheme.

INTRODUCTION

Power electronic devices are being deployed in distribution networks for various applications. They include integration of Distributed Energy Resources (DER), electronic on-load tap changers, solid-state fault current limiters and Soft Open Points (SOP) [1]–[3]. Currently, power electronic devices used to implement Medium Voltage (MV) Direct Current (DC) links is an area of interest for distribution engineers [4], [5]. A DC link is implemented using two Voltage Source Converters (VSCs) connected along a distribution network, as illustrated in Fig. 1. The two VSCs are installed either Back to Back or at different geographical locations.

SP Energy Networks (SPEN) are currently deploying a DC link in a distribution network in North Wales. This pilot project will demonstrate a flexible method for reinforcing a distribution network by converting alternating current (AC) circuits to DC operation. One VSC will be located in Llanfair PG substation on Anglesey (Island) and the other in Bangor substation in Wales (Mainland).

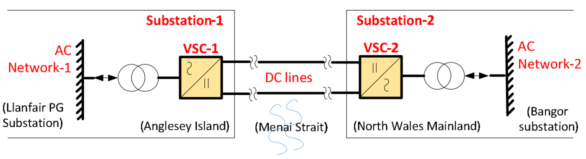

Fig. 1 Functional representation of a MVDC link (E.g. Anglesey-Bangor DC link)

This paper describes the operation of a DC link in an MV distribution network, considering its salient similarities and differences to a High Voltage (HV) DC link. Key drivers and the challenges of deploying MVDC in the existing medium voltage network were investigated. A model of an MVDC link was developed in PSCAD/EMTDC. Simulations were carried out for normal and faulted condition of the AC network. Case studies were used to illustrate some of the benefits and the challenges highlighted in this paper.

MVDC LINK

The VSC technology used for MVDC has some similarities to HVDC but simpler (e.g. two level) converters can be used for application at medium or low voltage. Multilevel topologies are predominant at higher voltage levels. Although multilevel converters can be used for lower voltages, direct scaling of HVDC link may not be economic for MVDC applications [3].

In its simplest two level form, each VSC has six arms of IGBTs connected across a capacitor, in a bridge configuration. The IGBTs in the arms are commutated to control the flow of current. Commutation can then be controlled using pulse width modulation (PWM). Smooth voltages are generated at the VSC terminals using low pass filters [6]. The capacitors limit the ripple in DC current and provide for decoupled real power (*P*) exchange between VSCs.

P transfer through the VSC is achieved by controlling the phase angles of the converter terminal voltage with respect to the grid connection point. Transfer of reactive power (*Q*) is achieved by controlling the amplitude of voltage at the converter terminal with respect to the voltage at the grid connection point.

Control of an MVDC link

Each VSC is equipped with a separate control system. Classical vector-control is a common control technique, since it allows the use of linear simple controls using proportional-integral (PI) controllers. This is achieved by transforming the three-phase (a, b, c) network quantities to a synchronously rotating reference frame (d, q, 0) using Parks transformation. Operation of the converters is synchronised to the grid using an angular frequency ω, obtained using a phase locked loop (PLL) [7]. The phase angle of the rotating frame is selected such that the resultant θ maintains the quadrature axis voltage (V_q) at zero.

The classical vector-controller has a cascaded control system, which includes a power (outer) and a current (inner) control loop as shown in Fig. 2. The power loop produces the direct (i_d*) and quadrature (i_q*) current reference signals for the current loop. PI controllers regulate active power (P) or DC voltage (V_{dc}) through the direct axis variable and reactive power (Q) or AC voltage (V_{ac}) through the quadrature axis variable. Switch *S1* is used to select the mode of operation between Active Power Control (APC) or Direct Voltage Control (DVC). Similarly, the Reactive Power Control (RPC) or Alternating Voltage Control (AVC) is selectable through switch *S2*. Therefore, the VSC control modes are switchable between the P-Q, V_{dc}-Q, V_{dc}-V_{ac} and P-V_{ac} modes.

The inner current loop regulates the current references values i_d* and i_q*, received from the power loop. Decoupling signals are included to eliminate cross-coupling dynamics. The summation of the current loop PI controller outputs and the decoupling terms produce the voltage reference signals V_d* and V_q*. These reference signals are converted back to three phase quantities using inverse Parks transformation. They are then fed to the modulation/firing blocks of the IGBTs to generate desired converter terminal voltage.

Sustaining the DC voltage ensures the balance of active power flow through the MVDC link. Therefore, either VSC1 or VSC2 can control V_{dc} for the proper operation of the link. However, both VSCs cannot control the DC link voltage simultaneously as this may lead to an undesired oscillation about the set point [7].

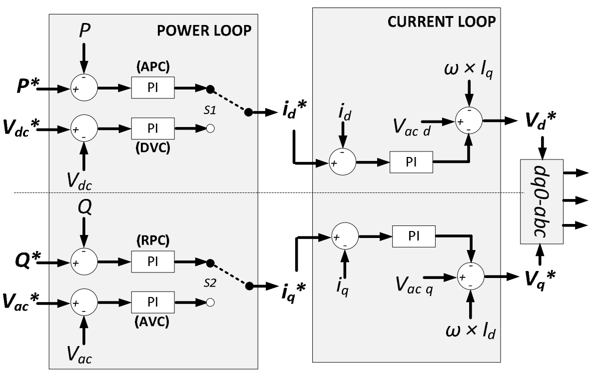

Fig. 2 VSC Controller in an MVDC link

BENFITS AND KEY DRIVERS OF MVDC

Operational flexibility of VSC

Each VSC can operate in all four quadrants of the P-Q plane transmitting P and Q in either direction up to its maximum rated power (S) capacity. The network operator has the flexibility to select the operating modes (P-Q, V_{dc}-Q, V_{dc}-V_{ac} and P-V_{ac}) and specify the corresponding power, voltage set points (P*, Q* and V_{ac}*). The set points can be changed continuously or in steps as per the network requirements [8]. The DC voltage (V_{dc}*) is usually fixed for an MVDC link design.

Utilization of cables

MVDC link is an effective network reinforcement method for distribution networks. During transfer of AC power, the overheating of outer layer due to non-uniform current distribution within a conductor is called skin effect [9]. The skin effect does not apply for DC power transfer due to non-oscillating nature of the direct current. Therefore, full cross section of the conductor is utilized during DC power transfer.

Fault levels

MVDC links enable the connection of two networks while only modestly increasing the fault levels of the individual networks. Furthermore, the two networks could be operating at different frequencies and phase angles. The two networks remain electrically decoupled during real and reactive power transfer through the MVDC link. Thus, MVDC allows higher connectivity of DERs through better load sharing in a distribution network.

CHALLENGES AND INHIBITORS OF MVDC

Efficiency

In general, power electronics devices operate at lower efficiency compared to traditional network equipment of comparable rating. A typical 230kVA DC link operates at a full load efficiency of 95.9%, including the auxiliary devices associated with its operation. This is 3% lower than the efficiency of a 250kVA transformer [2]. In medium voltage application, power electronic converters can have a higher power density (expressed in kW/m^3 or kW/kg) compared to a network transformer of similar ratings. Consequently, the heat dissipation and associated losses are higher. This is not the case in HVDC due to the large clearance needed at high voltages. Thus, cooling arrangements cannot be scaled down from a HVDC configuration and need to be designed specific to the application.

Isolation transformer winding arrangement

In HVDC applications, it is common to use a star-delta isolation transformer, with star winding connected to the AC network and delta winding to the converter. The neutral point of the star windings is connected to ground, either directly or via a resistor to control fault current levels. Shunt reactors are installed (grounded either directly or via a resistor) on the converter side. This provides a ground reference point to the DC side and a fault current path in the event of a DC fault. In HVDC applications, the choice of isolation transformer winding reflects the converter topology and the cost of insulation on the HV network.

However, this is not necessarily the case for MV networks. It is possible to use a delta-star transformer, with the star winding connected to the converter side. The star point is grounded via a resistor to limit the level of fault current. This combination avoids the need for separate ground reference point on the converter side. In addition, this grounding arrangement will not contribute to the zero-sequence currents during a fault in the AC network, since the majority of faults in a distribution network are ground faults; this arrangement may prove beneficial.

Currently, there are no standards or guidelines for the isolation transformer. It is therefore important to investigate the optimum winding/grounding arrangement of transformers to be used in MVDC applications.

Protection of distribution network

One of the challenges of deploying an MVDC link on an existing distribution network is its impact on distribution automation schemes. The interaction between the MVDC link and the protection devices on conventional distribution networks is not clear. An MVDC link operates as a current source during an AC fault on the distribution network. This current may interfere with the detection and discrimination of AC system faults, since protection in distribution networks is largely current based. It is therefore important to include the MVDC link into the network fault analysis to achieve its co-ordinated operation with the existing distribution automation scheme.

MODELLING OF AN MVDC LINK

Modelling of an MVDC link was undertaken based on the average model shown in Fig. 3. It employs a switched equivalent circuit of an IGBT bridge, with decoupled AC and DC sides. The AC side is modelled as a three phase voltage source ($E_{1(abc)}$ and $E_{2(abc)}$), whereas the DC side is modelled as a current source in parallel to a capacitor maintained at V_{dc}. The direct current (I_{dc}) flow represents the real power transfer between the VSCs.
The modulation index (m) is realized through a functional equivalent equation shown in Eq. 1. The converter terminal voltages are computed as a function of the m and $V_{dc.}$ as shown in Eq. 2.

$$m = V_{d\,Ref}\left(\frac{2}{V_{dc}}\right) \qquad (1)$$

$$E_k = m\left(\frac{V_{dc}}{2}\right);\ \text{where } k = a,b,c \qquad (2)$$

The average model using switched equivalent circuit is sufficient for this study as it describes the steady state and the dynamic behaviour of the VSC with sufficient accuracy [7].

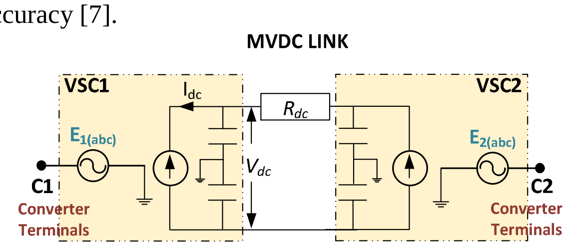

Fig. 3 Average model of an MVDC link

TEST NETWORK

Fig. 4 shows the test network simulated on PSCAD/ EMTDC. It consists of two distribution networks connected through an MVDC link. The MVDC link was rated at 6MVA. The DC link voltage was maintained at ±17.5kV (symmetrical monopole).
Representative generic 11kV UK distribution network models was used in this study [10]. AC networks 1 and 2 were modelled identically with identical devices and line characteristics. The AC network is fed from a delta-star 33/11.5kV, 15MVA grid transformer through a circuit breakers (CB_{1A} and CB_{1B}) in normally closed position. The transformer is grounded at its star point. The AC network consists of three 1km sections. The line impedance (Z_g) of each section is 0.164+j0.082 Ω/km. Lumped loads (L_{1A}, L_{1B} and L_{2A}, L_{2B}) of 1MW/ph were connected at each bus bar. G1 is the grid connection point of the MVDC link to AC network 1. G2 corresponds to grid connection point for AC network 2. A star-delta transformer (Tc1 and Tc2), grounded at its star point was used as an isolation transformer at terminals G1 and G2. Each VSC is connected to their respective isolation transformer through an inductor L=0.5H, to perform power control and filter the VSC output current.

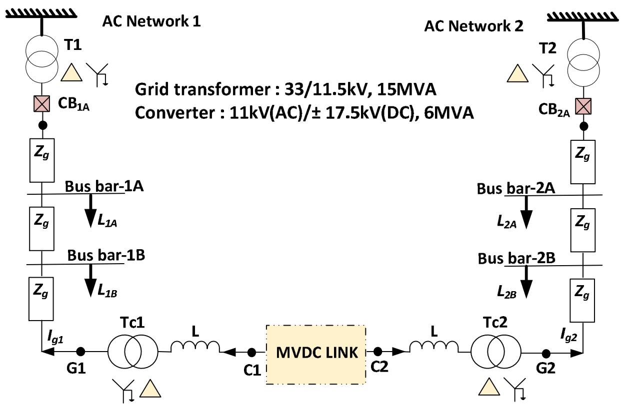

Fig. 4 Test network with MVDC link

CASE STUDIES

The following assumptions were made for the simulations.

1. VSC1 was operated in *P-Q* and VSC2 was operated in V_{dc}-Q control mode
2. No loads or DERs were connected to the DC cables.
3. The time needed for AC fault detection is neglected.
4. There were no faults within the MVDC link.

Case 1: Normal operation

This case illustrates the independent control of *P* and *Q* by the MVDC link during unfaulted operation. Simulations were carried out for various set points of the MVDC link, under normal network condition. (P_1*, Q_1*) are real and reactive power set points for VSC1. (V_{dc}*, Q_2*) are DC voltage and reactive power set points for VSC2.
The direction of power flow from AC Network- 1 to AC Network-2 was considered as positive throughout the simulation. The set points were changed in steps, as shown in Table-1.

Table 1. Set points (P_1, Q_1*) and (V_{dc}*, Q_2*) during normal operation*

Time	P_1* (MW)	Q_1* (MVAr)	V_{dc}* (kV)	Q_2* (MVAr)
t =0 s	2	-0.5	35	0.5
t =1 s	0	-0.5	35	0.5
t =2 s	0	0.5	35	-1.5
t =3 s	-1	0.5	35	-1.5
t =4 s	-1	-1.5	35	1
t =5 s	-1	-1.5	35	1

Fig. 5 shows the real and reactive power (P_1 and Q_1) through grid connection point G1, and Fig. 6 shows (P_2 and Q_2) through G2, under normal network conditions. The magnitude of *P* flow through both the terminals was equal throughout the simulation. However, the *Q* flow through one terminal was independent of the *Q* flowing through the other terminal. From the curves, it is clear that a VSC allows independent control of *P* and *Q* flow in either direction of the DC link. Any value within the capacity of the device can be assigned to the set points. The *P* and *Q* set points can also be changed continuously during operation.

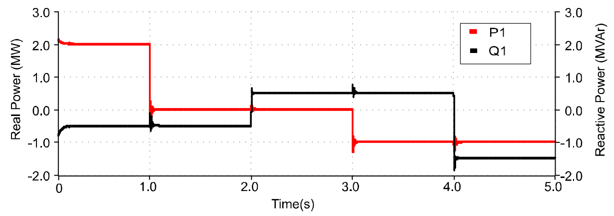

Fig. 5 P and Q flows through grid connection point G1 for different set points

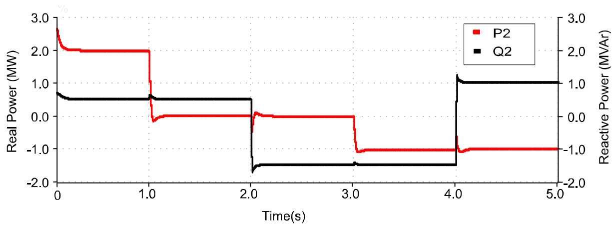

Fig. 6 P and Q flows through grid connection point G2 for different set points

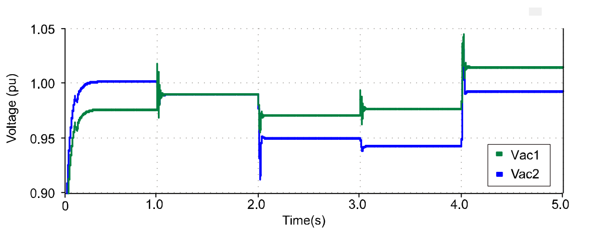

Fig. 7 Voltages at the grid connection points of MVDC link

Fig. 7 shows the voltages (V_{ac1} and V_{ac2}) at the grid connection points of the MVDC link (G1 and G2). The voltage at the terminal rises with an increase in *Q* injection into the network and conversely drops with removal of *Q* from the network. In addition, a voltage rise was observed with increasing injection of P into the network. This can be seen at time *t* =1s and *t* =3s in Fig. 7. This is due to the resistance (*R*) to reactance (*X*) ratio of the network. In a distribution network, its value is relatively high ($R/X \approx 0.3$ at 33kV and ≈1 at 11kV), thus the effect of real power on voltage profile cannot be ignored [1].

Case 2: During a fault

The behaviour of the MVDC link during an AC network fault was investigated. Case 2 was studied under two subcases.

Case 2a: Faulted AC network.

This case illustrates the injection of current by the MVDC link into a faulted network.

A three-phase fault was simulated on bus bar-1A, at time t=1sec. The current (I_{g1}) flowing at the grid connection point (G1) was monitored. A suitable voltage reference signal was assumed to be available for the PLL.

The Fig.8 shows the three phase current waveform through the grid connection point of the faulted AC network. There is a significant increase in the current. It however saturates, since the IGBTs have a fixed current carrying capacity. Normally the maximum currents trough the IGBTS are fixed at 1.4 times its rated current [11].

The fault current flowing in the network will be different with the inclusion of a MVDC link at the end of the network. The current injected by the MVDC link could trigger the protection device of the network device.

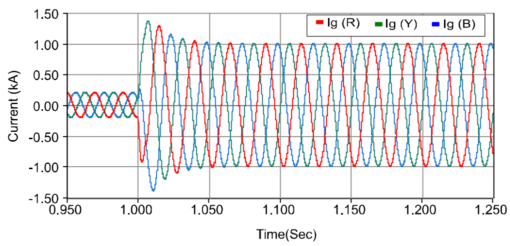

Fig. 8 Dynamic response of the current injected from MVDC link after a fault at t=1s

Case 2b: Unfaulted AC network.

This case illustrates the decoupled nature of the two networks connected through a DC link.

A three-phase fault was simulated on bus bar-1A, at time t=1sec. VSC connected to the faulted network (VSC1) was blocked, immediately after detecting the fault. The Q_2* was increased by 0.5MVAr at *t*=3s and 4s. The real and reactive power flow at the grid connection point (G2) was monitored. The relevant fault detection mechanism at G1 was assumed to be in place.

The Fig. 9 shows the *P* and *Q* flows through G2. There was no real power exchange across the MVDC link following a fault, since the VSC1 was blocked. However, the reactive power injection to the healthy AC network was unaffected. Q_2 rises in steps of 0.5MVAr corresponding to the change in Q_2*, regardless of the fault on AC network 1. The voltage of AC network 2 (V_{ac2}) also changes corresponding to the changes in the value of *Q* injection.

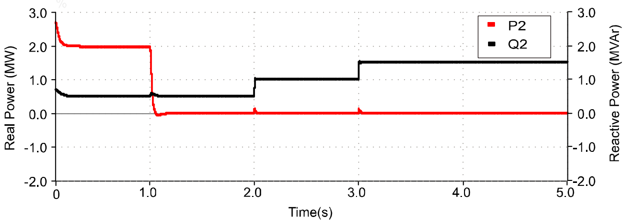

Fig. 9 P and Q flows through grid connection point G2 after a fault at t=1s

CONCLUSION

Existing distribution networks are facing rapid growth of demand and generation. MVDC can be a flexible method for reinforcing the distribution network. It is able to facilitate maximum utilization of the available network and support future integration of renewable generation resources.

The dynamic operation of an MVDC link, under normal and faulted network condition was investigated. The simulation results show that the MVDC can provide flexibility in a distribution network by decoupling real (*P*) and reactive (*Q*) power flows through the link, under normal operation. However further analysis is needed to understand its interaction with existing network devices during a fault. It is important to include the MVDC link into the network fault analysis to achieve its co-ordinated operation with the existing distribution automation.

Acknowledgments

The authors gratefully acknowledge the UK/India HEAPD project and Angle-DC project.

REFERENCES

[1] T. Green and N. Jenkins, "HubNet Position Paper Series Issues for Distribution System Operation at 2030," 2014.

[2] R. Silversildes, T. Green, and T. Luth, "HubNet Position Paper Series - Power Electronics in Distribution System Management - Version 0.6," 2014.

[3] J. M. Bloemink and T. C. Green, "Benefits of Distribution-Level Power Electronics for Supporting Distributed Generation Growth," *IEEE Trans. Power Deliv.*, vol. 28, no. 2, pp. 911–919, Apr. 2013.

[4] Scottish Power Energy Networks, "Electricity NIC submission: SP Energy Networks – ANGLE-DC," 2016. [Online]. Available: https://www.ofgem.gov.uk/publications-and-updates/electricity-nic-submission-sp-energy-networks-angle-dc.

[5] G. Bathurst, G. Hwang, and L. Tejwani, "MVDC - The New Technology for Distribution Networks," *11th IET Int. Conf. AC DC Power Transm.*, no. Dc, pp. 1–5, 2015.

[6] U. Axelsson, A. Holm, and C. Liljegren, "Gotland HVDC light transmission-World's first commercial small scale DC transmission," in *CIRED Conference*, 1999, no. May, p. 5 pages.

[7] A. Yazdani and R. Iravani, "Grid Imposed Frequency VSC system: Control in dq-Frame," in *Voltage-sourced converters in power systems: modeling, control, and applications*, John Wiley & Sons, 2010, pp. 204–245.

[8] European Commission, "COMMISSION REGULATION (EU) 2016/1447 of 26 August 2016. Establishing a network code on requirements for grid connection of high voltage direct current systems and direct current-connected power park modules," *Off. J. Eur. Union*, no. L 241, pp. 1–65, 2016.

[9] B. M. (Birron M. Weedy, B. J. Cory, N. Jenkins, J. B. Ekanayake, and G. Strbac, *Electric power systems*, 5th ed. Wiley, 2012.

[10] G. Ault, "United kingdom generic distribution system (UKGDS)," in *DTI Centre for Distributed Generation and Sustainable Electrical Energy*, 2010.

[11] J. M. Bloemink and M. R. Iravani, "Control of a multiple source microgrid with built-in islanding detection and current limiting," *IEEE Trans. Power Deliv.*, vol. 27, no. 4, pp. 2122–2132, 2012.